

RESEARCH MEMORANDUM

EFFECTS OF RATE OF FLAP DEFLECTION ON FLAP HINGE MOMENT

AND WING LIFT THROUGH THE MACH NUMBER

RANGE FROM 0.32 TO 0.87

By Thomas R. Turner

Langley Aeronautical Laboratory
Langley Field, Va.

Classification changed to

Unclassified

May 10, 1955

Authority Mr. J. W. Crowley

Change #2998

W. H. L.

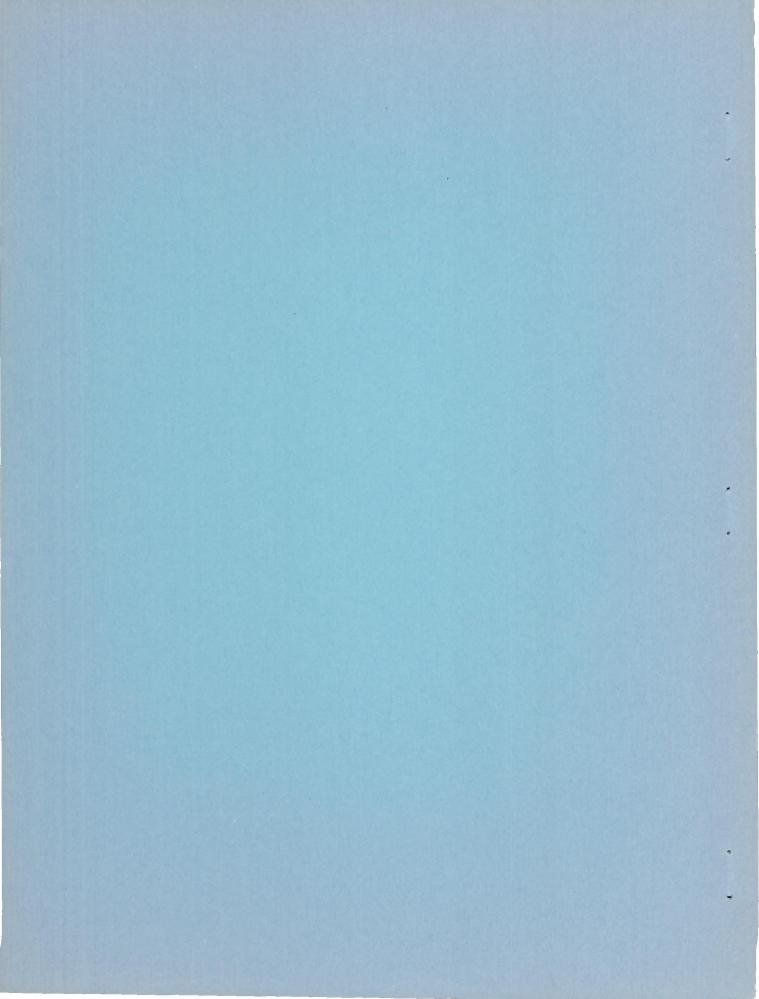
CLASSIFIED DOCUMENT

This material contains information affecting the National Defense of the United States within the meaning of the espionage laws, Title 18, U.S.C., Secs. 793 and 794, the transmission or revelation of which in any manner to an unauthorized person is prohibited by law.

NATIONAL ADVISORY COMMITTEE FOR AERONAUTICS

WASHINGTON

June 26, 1953



NATIONAL ADVISORY COMMITTEE FOR AERONAUTICS

RESEARCH MEMORANDUM

EFFECTS OF RATE OF FLAP DEFLECTION ON FLAP HINGE MOMENT

AND WING LIFT THROUGH THE MACH NUMBER

RANGE FROM 0.32 TO 0.87

By Thomas R. Turner

SUMMARY

An investigation has been made to determine the effect of rate of flap deflection on flap hinge moment and wing lift at Mach numbers from 0.32 to 0.87 with the Reynolds number varying from approximately 1.0 to 2.3 \times 10 6 . The wing had an aspect ratio of 4, a taper ratio of 0.6, NACA 65A006 sections, and zero sweep of the 75-percent-chord line. The wing was fitted with a 25-percent-chord full-span plain flap. The flap-deflection rate varied from 0° to 1.17° per chord length of travel.

For the rate of flap-deflection range investigated the hinge-moment coefficient was practically independent of rate of flap deflection. The lift coefficient was practically independent of rate of flap deflection with two exceptions; namely, at a Mach number of 0.52 at 12° angle of attack and at a Mach number of 0.72 at 8° angle of attack.

INTRODUCTION

The present-day airplane with its high control forces has compelled the designer to resort to boosters to enable the pilot to control the airplane. The ability of these boosters and similarly the ability of missile control mechanisms to deflect control surfaces at rather high rates has raised the question of the effect of rate of control deflection on control characteristics. This effect could become especially important if the main lifting surface were at a relatively high angle of attack and the rate of deflection influenced the formation of separated or stalled air flow. It is conceivable for this condition that the hinge moment could get large enough to cause damage to the system before the mechanism had time to reverse and reduce the load.

There are considerable static control force and control effectiveness data available throughout the subsonic Mach number range; however, there is very little dynamic control force data available throughout this Mach number range.

It is the purpose of this paper to present the data obtained in an investigation of the effect of rate of flap deflection on flap hinge moment and wing lift. The wing used had an aspect ratio of 4, a taper ratio of 0.6, NACA 65AOO6 sections parallel to the plane of symmetry, and had zero sweep of the 75-percent-chord line.

The investigation covered a Mach number range from 0.32 to 0.98 for static condition of the flap and 0.32 to 0.87 for dynamic condition of the flap, with the Reynolds number varying from approximately 1.0 to 2.3×10^6 . The angle-of-attack range was from 0° to 20° and the flap angle varied from approximately 0° to approximately 60°. The rate of flap deflection varied from 0° to 1.17° per chord length of travel.

COEFFICIENTS AND SYMBOLS

$\mathtt{C}_{\mathtt{L}}$	lift coefficient, L/qS
Ch	hinge-moment coefficient, h/q2M'
L	lift, 1b
h	hinge moment, ft-lb
M'	area moment of semispan flap rearward of hinge line about hinge line, 0.00804ft^3
S	twice area of semispan model, 1.003 sq ft
Ъ	twice span of semispan model, 2.000 ft
c	mean aerodynamic chord of model, 0.512 ft
q	dynamic pressure, $\frac{\rho V^2}{2}$, lb/sq ft
М	average Mach number over span and chord of model
R	Reynolds number of wing based on \overline{c}
V	free-stream velocity, ft/sec

α angle of attack, trailing edge down positive, deg

 δ_{f} flap deflection, trailing edge down positive, deg

 $d\delta_{\rm f}/dt$ rate of flap deflection, deg per sec

 $\left(\frac{\overline{c}}{v}\right)\left(\frac{d\delta_f}{dt}\right)$ flap-deflection parameter, deg per chord length of travel

$$c^{\Gamma \alpha} = \frac{\alpha}{9c^{\Gamma}}$$

$$C_{h_{\delta}} = \frac{\partial C_{h}}{\partial \delta}$$

MODEL AND APPARATUS

This investigation utilized a semispan model mounted on a reflectionplane plate that was installed on one of the test-section side walls of the Langley high-speed 7- by 10-foot tunnel.

The model was constructed of steel with the 75-percent-chord line perpendicular to the plane of symmetry, and had an aspect ratio of 4.0, a taper ratio of 0.6, and NACA 65A006 sections parallel to the plane of symmetry. The sweep of the quarter-chord line was 7.13° . The model was fitted with a full-span 0.25-chord plain flap attached to the wing with four hinges with a flap gap of 0.05 percent of the wing chord. These and other details of the model are shown in figure 1.

The 40.5-inch by 60-inch reflection-plane plate with circular-arc camber was supported 4 inches from the tunnel side wall to bypass the tunnel-wall boundary layer (fig. 1). This particular plate gave the best Mach number gradients of three different curvature plates investigated. The streamwise velocity gradient over the center line of the plate surface is shown in figure 2. The spanwise Mach number gradient was approximately 0.01 in 12 inches, the semispan of the model. The test Mach number was the average Mach number over the span and chord of the model.

The model was mounted to a balance designed to measure instantaneous lift, hinge moment, and flap deflection (fig. 3). The lift part of the balance consisted of a lift platform connected to a heavy base plate with

two parallel flexure plates designed to allow the lift platform to move approximately 0.002 inch for 500 pounds lift. The natural frequency of the lift platform thus mounted was approximately 500 cycles per second, a frequency well above the flap oscillation frequency. The lift platform was connected to an electrical displacement gage through a mechanical multiplier arm giving several sensitivities to the lift measuring gage. The wing was bolted to the lift platform in such a manner that the angle of attack could be changed by loosening two bolts and rotating the wing about the flap hinge axis. The flap was made with a 3-inchlong 7/16-inch-diameter shaft extending from the root end of the flap, an extension of the hinge axis. This extension shaft, through which the flap was driven, had a 1/2-inch-long section near the center turned down to 9/32-inch diameter. An electrical strain gage indicated hinge moment by measuring the twist in the reduced diameter section of the shaft. The position of the flap was measured by means of the slide wire shown in figure 3. The flap was forced to oscillate at the desired rate by a motor-driven cam designed to give zero acceleration for approximately 45° of a 61° total deflection with equal dwell periods at the upper and lower limits of deflection. This cam was designed for a previous investigation; however, its type of motion was thought to be satisfactory for the present investigation. The cam and motor drive details located on the underside of the balance base plate are shown in figure 4.

The data were recorded by means of a recording oscillograph. A trace of the tunnel dynamic pressure was recorded simultaneously with the other data in order to get the magnitude of the change in dynamic pressure as the flap was deflected through its cycle. The type of flap oscillation and a sample of the recordings with and without air flow are shown in figure 5.

The hinge-moment coefficients presented have been corrected for the wind-off variation of hinge moment with flap deflection shown in figure 5.

The model and reflection plane installed in the tunnel are shown in figure 6. The balance was mounted to the side of the tunnel in an airtight box to minimize the effect of leakage around the root of the model. To reduce the leakage further, a sponge rubber seal was placed between the butt of the wing and the back of the reflection plane turntable.

The variation of Reynolds number with Mach number for this investigation is presented in figure 7.

RESULTS AND DISCUSSION

The variation of lift coefficient and hinge-moment coefficient with flap deflection is presented in figure 8. In general, rate of flap deflection had very little effect on the variation of lift coefficient with flap deflection; however, there are two exceptions that should be noted. At a Mach number of 0.72 and an angle of attack of 80 (fig. 8(g)), the lift-coefficient curve for the static flap condition decreases about two-tenths at about 46° flap deflection. The flap in the dynamic conditions gave two $C_{
m L}$ curves, one essentially agreeing with the static curve, the other somewhat lower and fairing into the static curve beyond the break. It appears that this combination of model, Mach number, and angle of attack permits two flow conditions and that the resulting lift curves might fall along either the upper or lower curves shown in figure 8(g). The original record of the flap oscillating through several cycles for this condition is shown in figure 5. The second exception is at a Mach number of 0.52 and an angle of attack of 120 where the lift coefficient is a function of the rate of flap deflection, the lift coefficient increasing with increasing rate of flap deflection for most of the flap-deflection range (fig. 8(i)).

Flap hinge-moment coefficient for all conditions was independent of rate of flap deflection for all practical purposes (fig. 8). In the two cases in which the lift was considerably influenced by rate of flap deflection and flow conditions (figs. 8(g) and 8(i)), the hingemoment coefficient curve was unaffected by these same conditions.

A typical plot showing the lift coefficient and hinge-moment coefficient as the flap is deflected through a complete cycle is presented in figure 9. There is some difference between the curves for the extending flap and the curves for the retracting flap.

The curves of lift coefficient plotted against angle of attack (fig. 10) show an increase in $C_{\rm L_{C\!\!\!\!/}}$ with Mach number up to a Mach number of 0.87 and a decrease with further increase in Mach number. Mach number had very little effect on $C_{\rm L_{max}}$ up to a Mach number of 0.87 but had considerable effect above a Mach number of 0.87, in that $C_{\rm L_{max}}$ increased with increased Mach number. These results are in qualitative agreement with results for a similar wing reported in reference 1.

The hinge-moment parameter $C_{h_{\bar 0}}$ increased with Mach number from -0.0095 at M = 0.32 to -0.0175 at M = 0.87 (fig. 11). The flap effectiveness parameter $C_{L_{\bar 0}}$ increased from 0.032 at M = 0.32 to 0.40 at M = 0.72 then decreased with further increase in Mach number.

These slopes were taken through $\,\delta=0^{\,\text{O}}\,$ for $\,\alpha=0^{\,\text{O}}\,$ and a static condition of the flap.

CONCLUSIONS

Results from wind-tunnel tests at Mach numbers from 0.32 to 0.87 of an aspect ratio 4, taper ratio 0.6 wing, with the 0.75-chord line unswept, fitted with a full-span 25-percent-chord plain flap have indicated that:

- 1. Flap hinge-moment coefficient was practically independent of rate of flap deflection from 0° to 1.17° deflection per chord length of travel.
- 2. Wing lift coefficient was practically independent of rate of flap deflection with two exceptions: (a) At a Mach number of 0.52 and angle of attack of 12° , the lift coefficient increased with increased rate of flap deflection for most of the lift range; (b) At a Mach number of 0.72 and an angle of attack of 8° , lift curves of different slopes and two different maximum lift-coefficient values were obtained, indicating the existence of two different flow patterns.

Langley Aeronautical Laboratory,
National Advisory Committee for Aeronautics,
Langley Field, Va.

REFERENCE

1. Turner, Thomas R.: Effects of Sweep on the Maximum-Lift Characteristics of Four Aspect-Ratio-4 Wings at Transonic Speeds. NACA RM L50Hll, 1950.

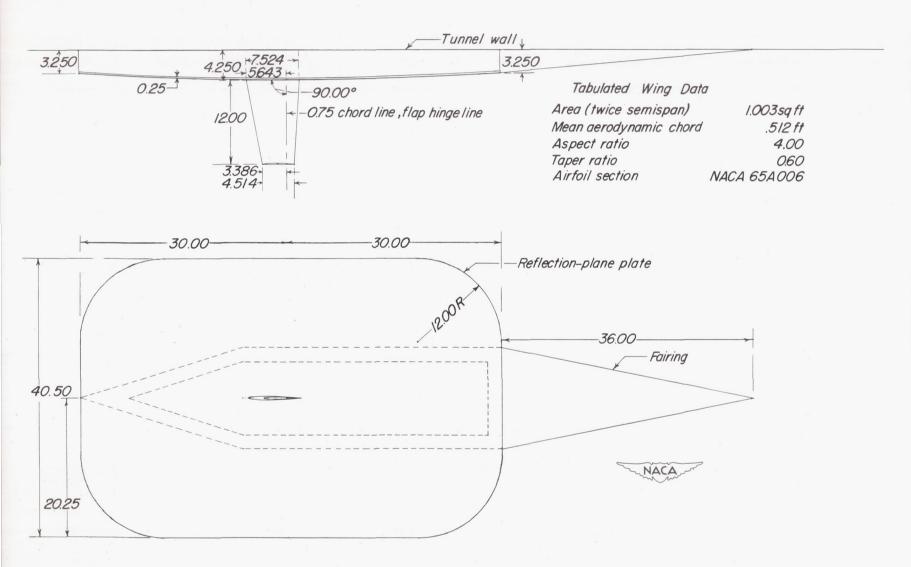


Figure 1.- Details of wing and reflection plane. Dimensions in inches.

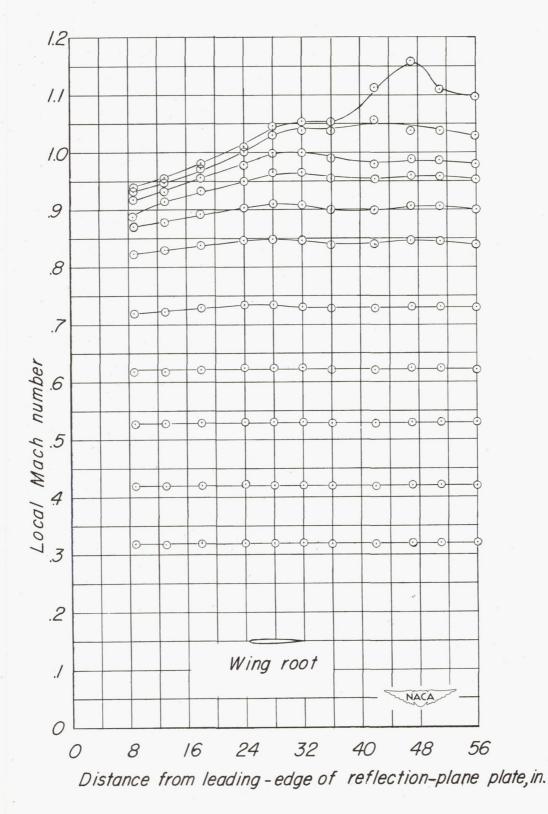


Figure 2.- Velocity distribution along center line of reflection-plane plate.

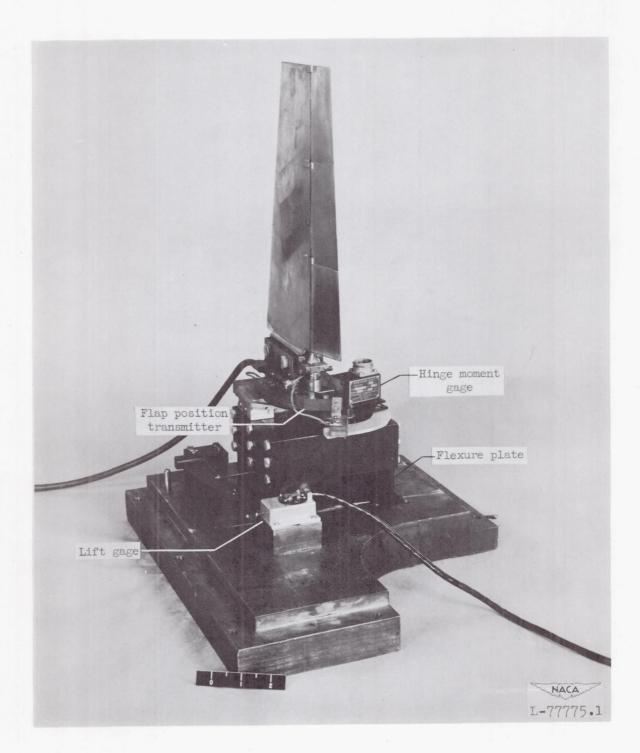
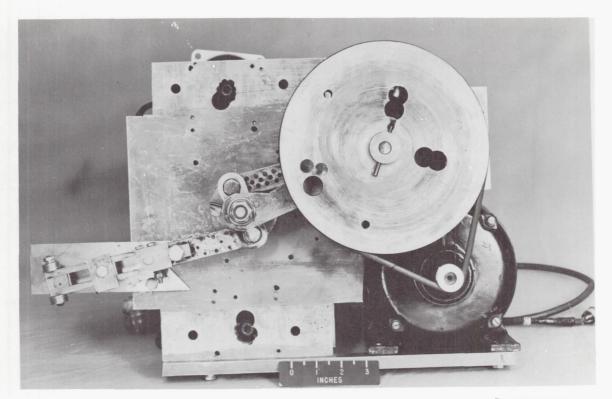


Figure 3.- Photograph of model and balance.



NACA L-69381

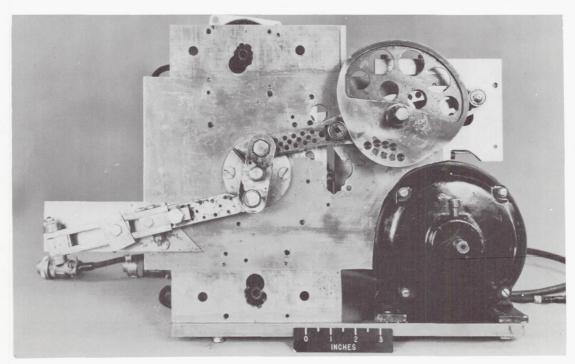


Figure 4.- Photograph of flap oscillating mechanism.



Wind off

Wind on

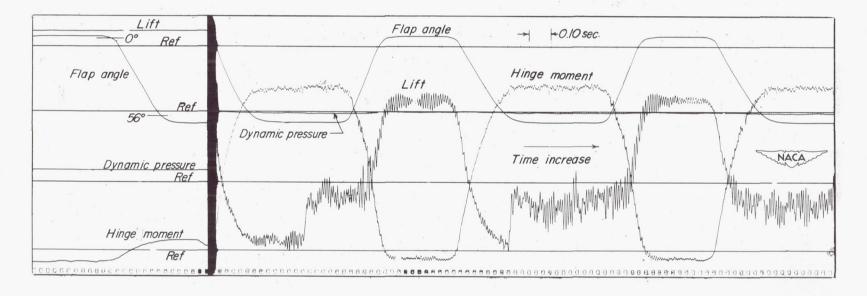


Figure 5.- A typical wind-off and wind-on record. M = 0.72; α = 8° .

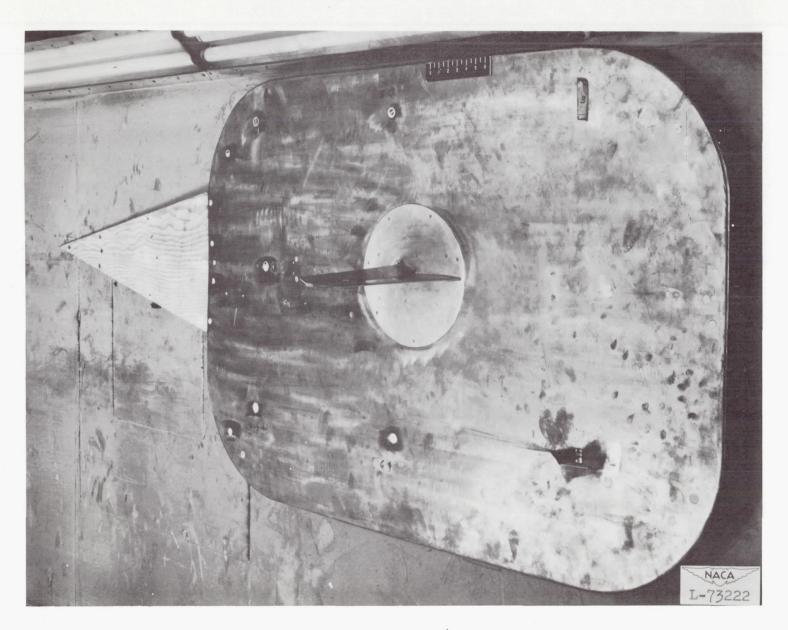
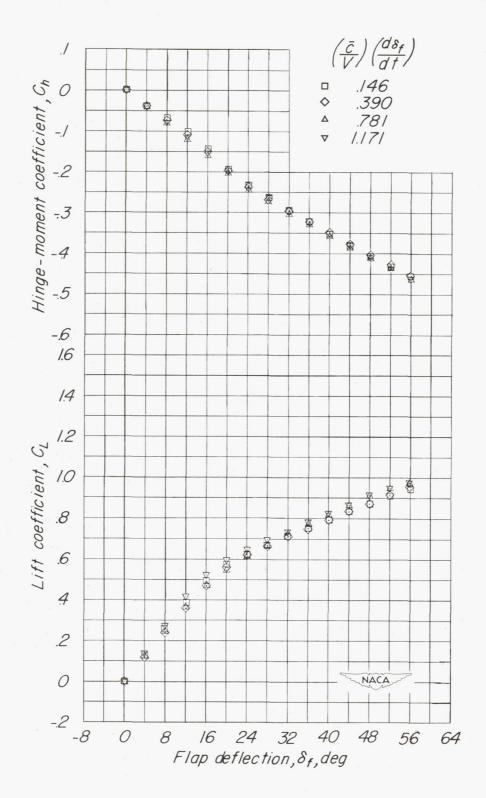


Figure 6.- Photograph of model and reflection plane mounted in the tunnel.

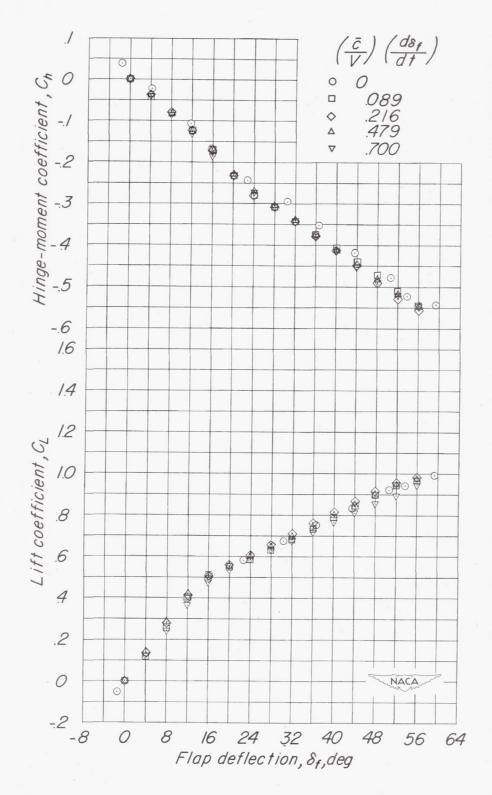


Figure 7.- Variation of Reynolds number with Mach number for the investigation.



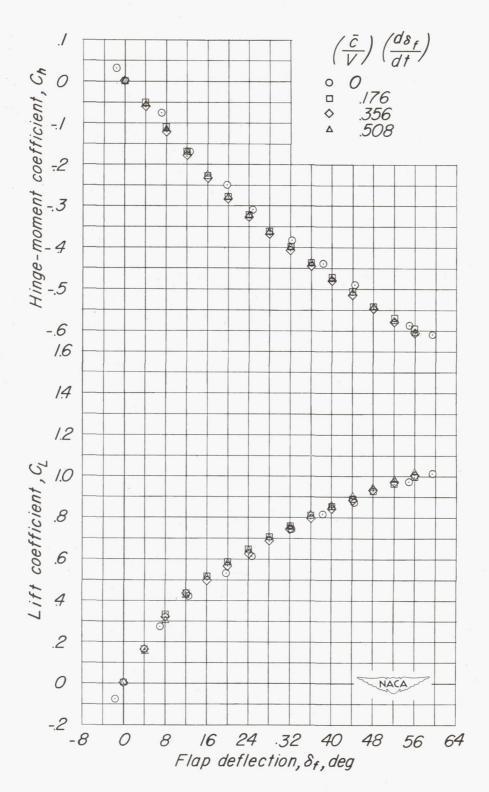
(a) $\alpha = 0^{\circ}$; M = 0.32.

Figure 8.- Variation of lift coefficient and hinge-moment coefficient with flap deflection.



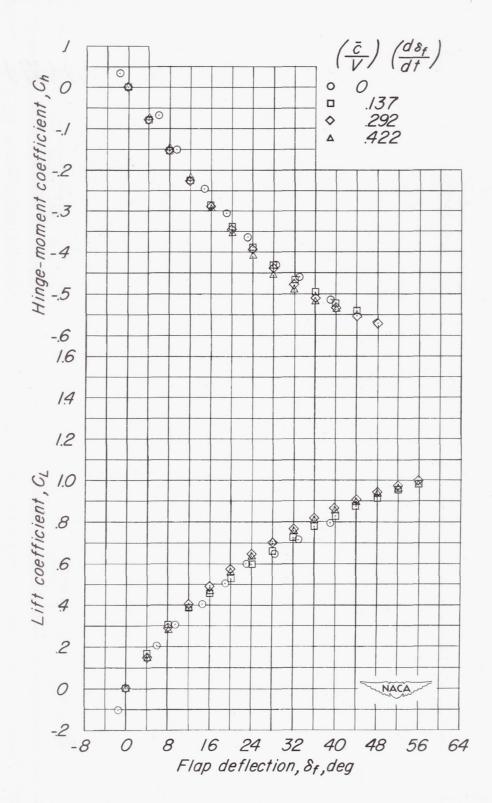
(b) $\alpha = 0^{\circ}$; M = 0.52.

Figure 8.- Continued.



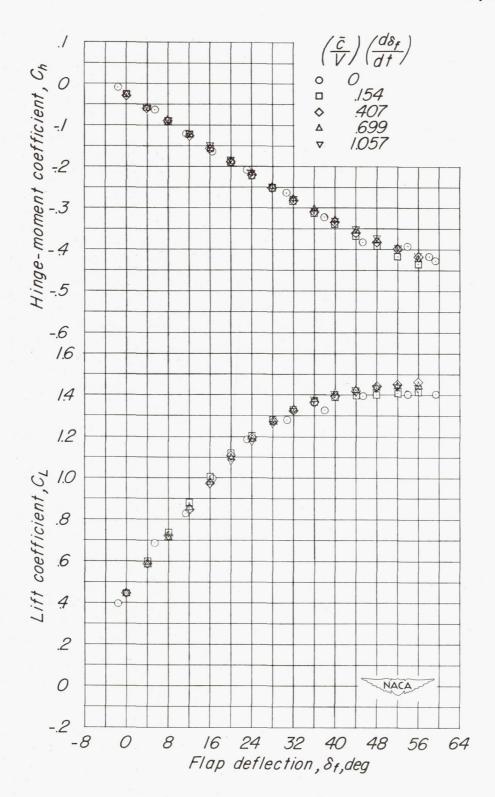
(c) $\alpha = 0^{\circ}$; M = 0.72.

Figure 8.- Continued.



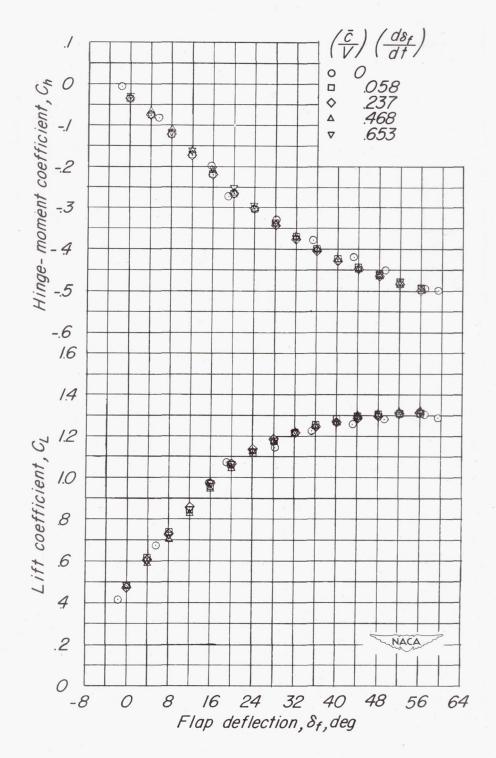
(d)
$$\alpha = 0^{\circ}$$
; $M = 0.87$.

Figure 8.- Continued.



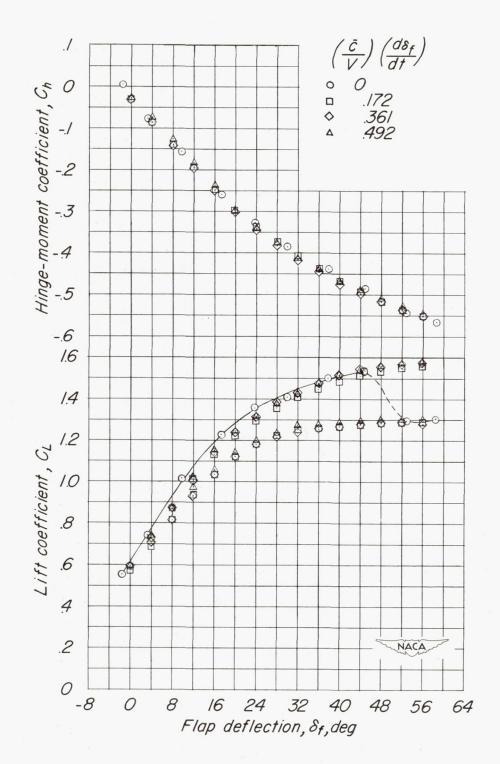
(e)
$$\alpha = 8^{\circ}$$
; M = 0.32.

Figure 8.- Continued.



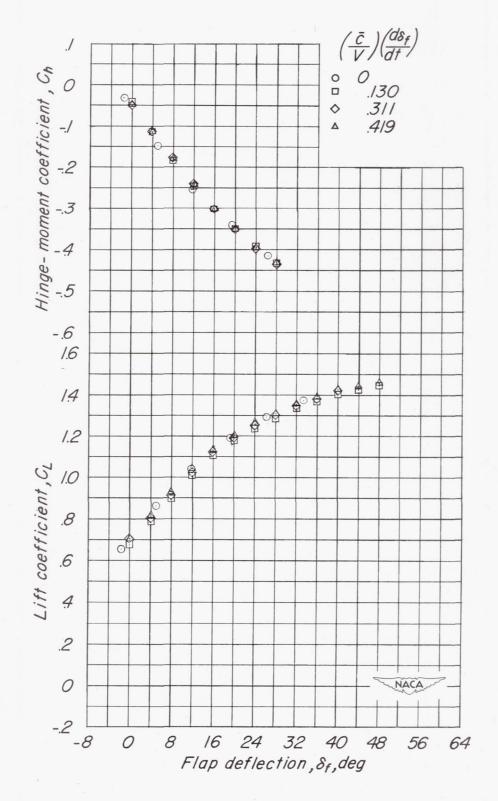
(f) $\alpha = 8^{\circ}$; M = 0.52.

Figure 8.- Continued.



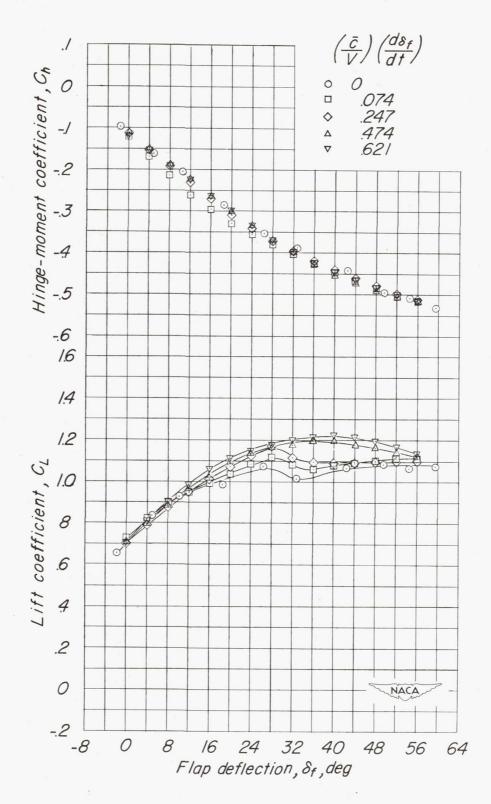
(g) $\alpha = 8^{\circ}$; M = 0.72.

Figure 8.- Continued.



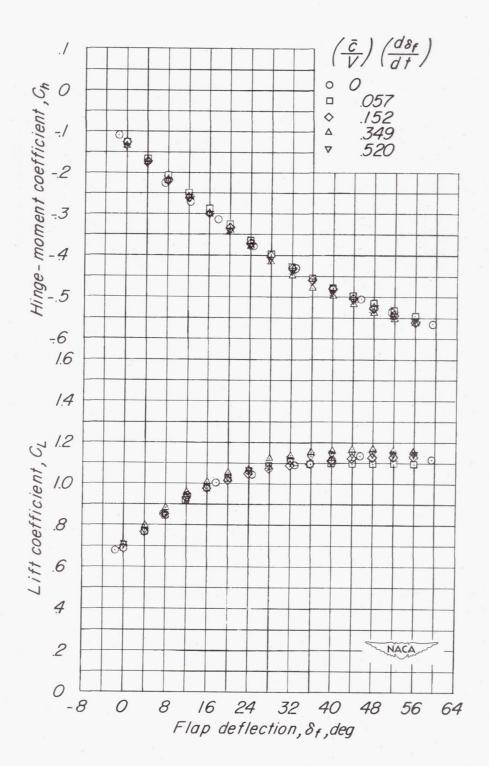
(h) $\alpha = 8^{\circ}$; M = 0.87.

Figure 8.- Continued.



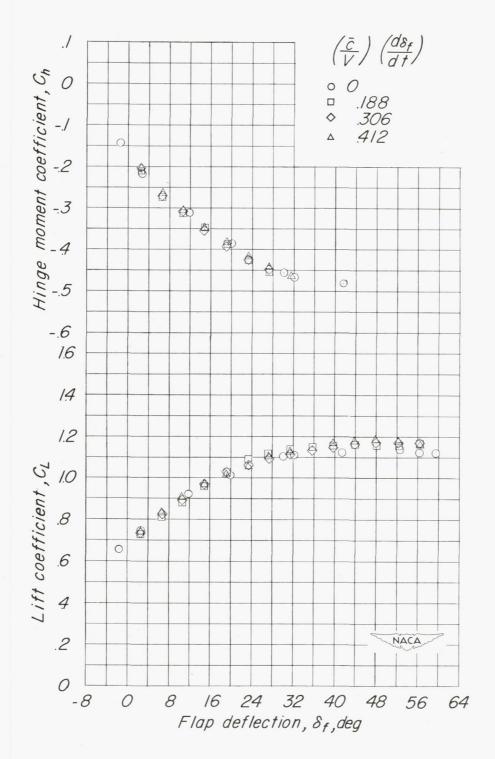
(i) $\alpha = 12^{\circ}$; M = 0.52.

Figure 8.- Continued.



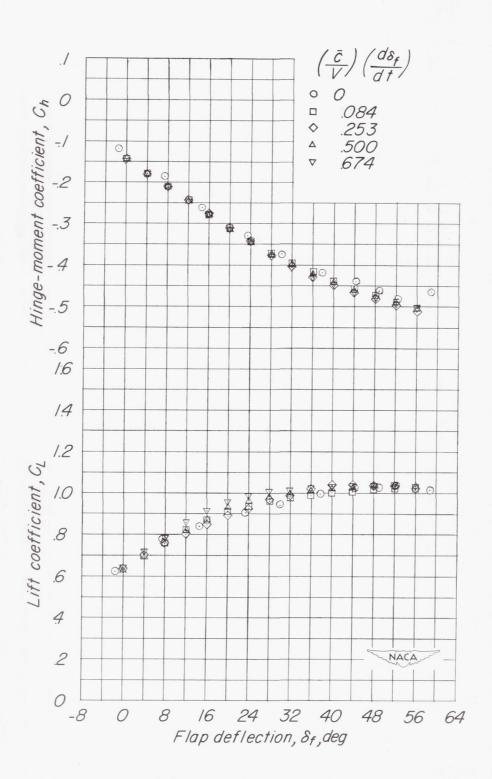
(j) $\alpha = 12^{\circ}$; M = 0.72.

Figure 8.- Continued.



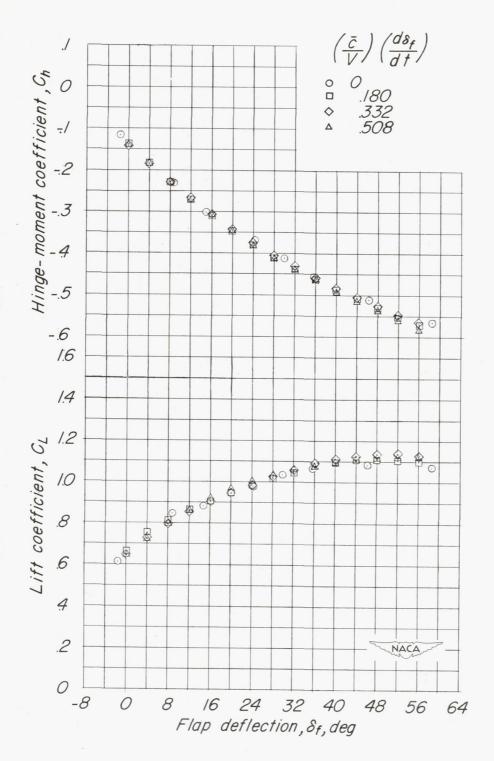
(k) $\alpha = 12^{\circ}$; M = 0.87.

Figure 8.- Continued.



(1) $\alpha = 16^{\circ}$; M = 0.52.

Figure 8.- Continued.



(m) $\alpha = 16^{\circ}$; M = 0.72.

Figure 8.- Concluded.

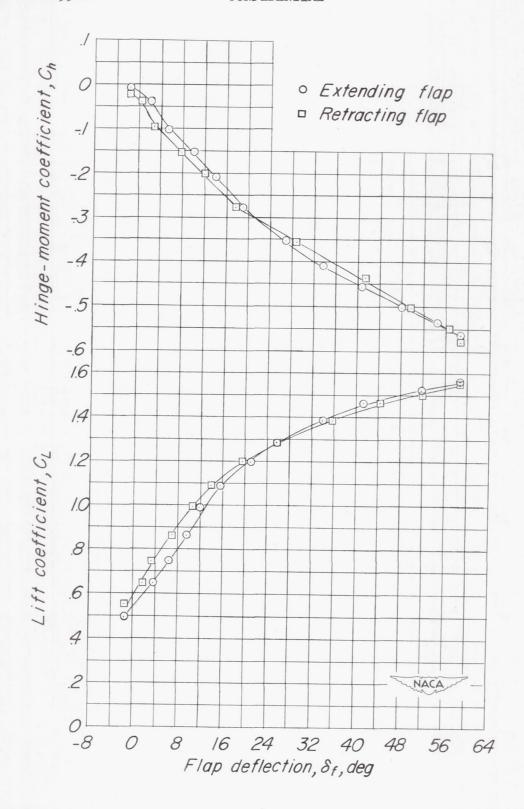


Figure 9.- A comparison of extending-flap and retracting-flap aerodynamic characteristics. $\alpha = 8^{\circ}$; M = 0.72; $\left(\frac{\bar{c}}{V}\right)\left(\frac{d\delta_f}{dt}\right) = 0.492$.

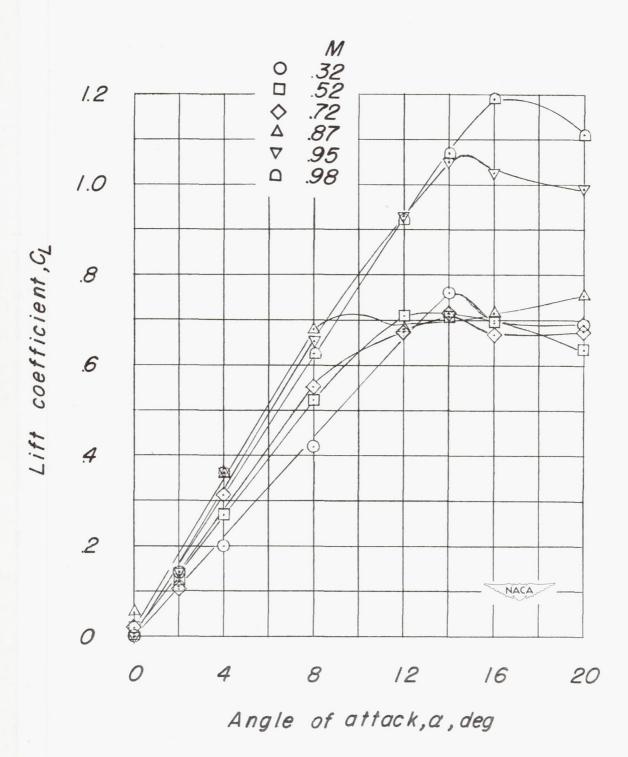


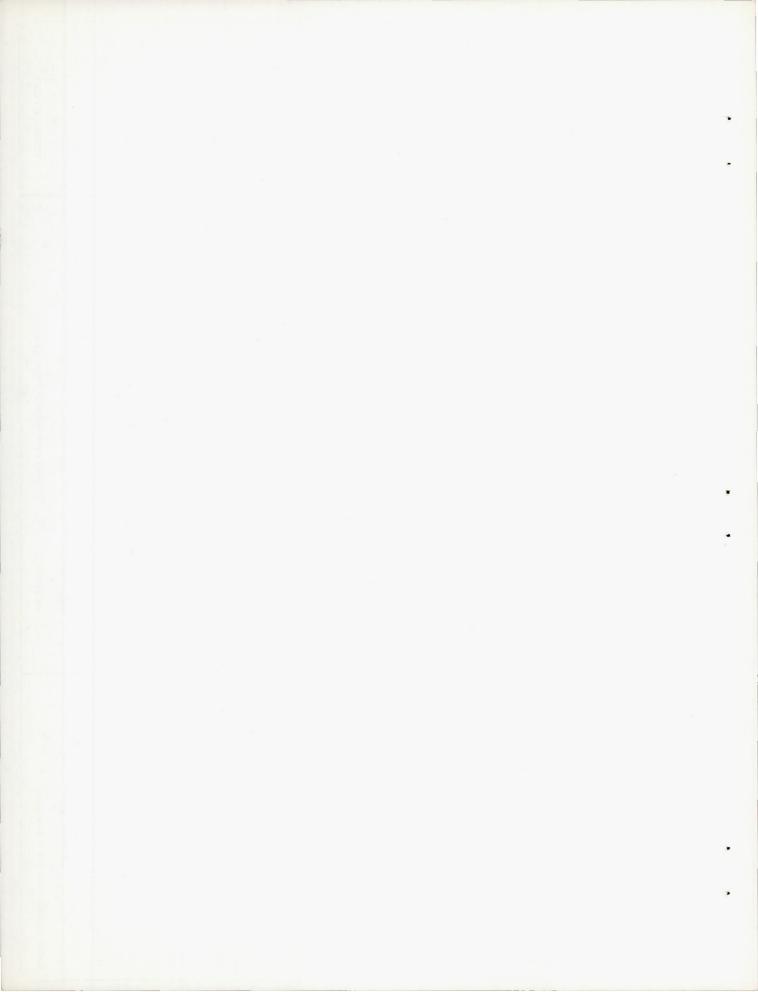
Figure 10.- Variation of lift coefficient with angle of attack. $\delta_{\rm f} = 0^{\rm O}$.

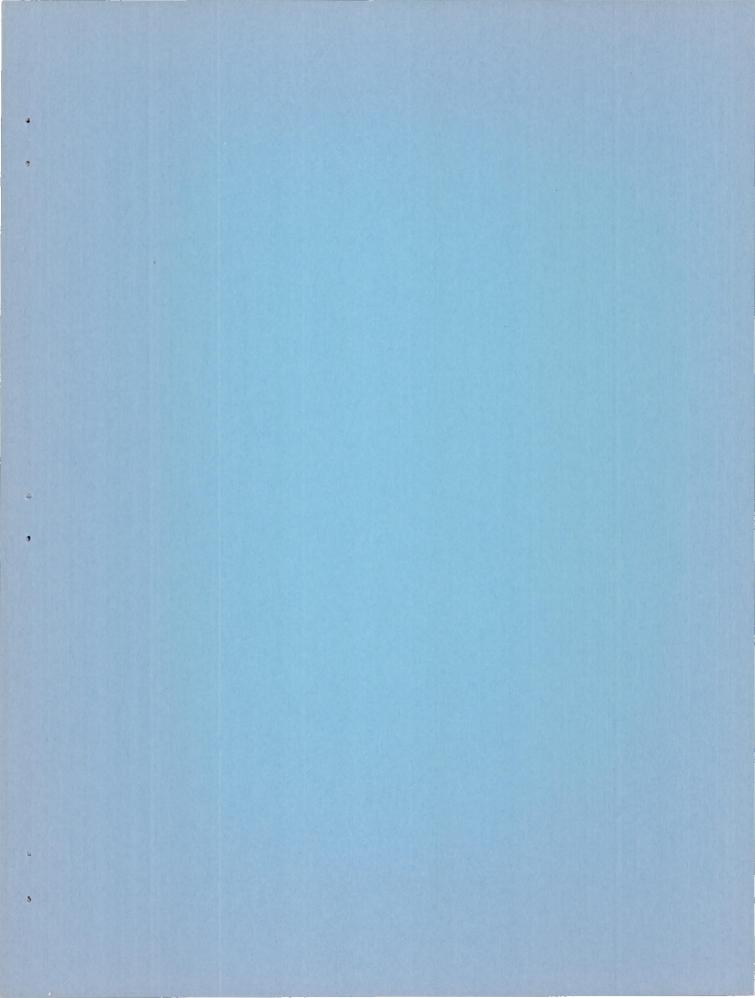
NACA RM L53Ell





Figure 11.- Variation of ${\rm C_{L_{\delta}}}$ and ${\rm C_{h_{\delta}}}$ with Mach number.





SECURITY INFORMATION CONFIDENTIAL